3-D elastic numerical modeling of a complex salt structure

Leigh House, Los Alamos Seismic Research Center/Los Alamos National Laboratory, Shawn Larsen, Lawrence Livermore National Laboratory, and J. Bee Bednar, Advanced Data Solutions*

Summary

Reliably processing, imaging, and interpreting seismic data from areas with complicated structures, such as sub-salt, requires a thorough understanding of elastic as well as acoustic wave propagation. Elastic numerical modeling is an essential tool to develop that understanding. While 2-D elastic modeling is in common use, 3-D elastic modeling has been too computationally intensive to be used routinely. Recent advances in computing hardware, including commodity-based hardware, have substantially reduced computing costs. These advances are making 3-D elastic numerical modeling more feasible. A series of example 3-D elastic calculations were performed using a complicated structure, the SEG/EAGE salt structure. The synthetic traces show that the effects of shear wave propagation can be important for imaging and interpretation of images, and also for AVO and other applications that rely on trace amplitudes. Additional calculations are needed to better identify and understand the complex wave propagation effects produced in complicated structures, such as the SEG/EAGE salt structure.

Introduction

There has been considerable recent interest in understanding elastic wave propagation and in best exploiting the information that shear waves provide because of two recent developments in exploration. First is increasing exploration of areas with complicated structures and large velocity contrasts, such as sub-salt. Second is the increasing availability of multi-component seismic data.

Qin, et al (1977) showed that even 2-D elastic simulations could be a powerful tool to correctly identify shear (converted) waves. They also showed that shear waves provide information to more reliably interpret seismic data from below salt. The greater reliability of their interpretation helped reduce the risks of exploring prospects below salt. If shear wave events are not properly identified, they can be misleading artifacts and lead to erroneous interpretations. In addition, since shear waves are more sensitive to the presence of fluids than compressional waves are, shear wave data may provide more reliable estimates of reservoir properties. Thus, reservoirs can be better understood and more reliably modeled and exploited.

Elastic wave modeling demands much more computer resources than are needed for acoustic wave modeling. More memory is needed because of the greater number of model parameters, and more computing time is required to carry out the computations. The additional variables introduced by going to elastic computations add a factor of 3-4 to both the memory and computing time needed. But, this factor alone is not the most important impact that results from going from acoustic to elastic simulations. The fact that shear wave velocities are lower than compressional wave velocities and their wavelengths are proportionally shorter means that elastic wave simulations generally require that the velocity model be specified on a finer spatial grid interval. That further increases the memory and computing time needed. The combined result of the additional elastic variables and the finer grid spacing required by elastic modeling is an overall increase in computing time by 25-100 times compared to acoustic model calculations.

The SEG/EAGE 3-D numerical modeling project (see Aminzadeh, et al, 1997) demonstrated that numerical modeling could be an important tool for testing and validating imaging methods. That project designed model structures to mimic complex, yet plausible, salt and overthrust geologic structures. Millions of simulated seismic traces were computed in these structures, in a *tour de force* of computing that harnessed the combined power of supercomputers in the U.S. and Europe. The result was a multi-terabyte data set that is available to researchers world-wide.

As powerful as the computing resources used by the SEG/EAGE numerical modeling project were, however, the project was only able to carry out acoustic wave calculations. The project was obliged to choose to carry out acoustic simulations because of the relatively high cost of the computing resources that were available at the time (about 5 years ago). Dramatic recent increases in computing resources, notably memory, computing speed, and storage space, make elastic wave computations, even in 3-D, more feasible. Development of computing clusters based on commodity-PC's has dramatically accelerated the rates of increase in computing capability and of decrease in cost. These trends are likely to continue, and will allow 3-D elastic wave calculations to be used more routinely, even by relatively small organizations.

To help emphasize the benefits of 3-D elastic wave simulations, we show the results of example calculations done in the SEG/EAGE salt model.

Method

3-D elastic computations were carried out using the modeling

code "E3D" (Larsen and Grieger, 1998). E3D is a finite difference modeling code that has been developed in a multi-year effort and has been successfully used in several different applications in addition to seismic reflection modeling. It is a well-documented and well-proven code. It includes many computational enhancements, such as propagating grid, static grid refinement, hybridization, parallelization, low-level optimizations, and surface topography (in 2-D). It can be used for 2-D or 3-D calculations, both elastic and acoustic. Elastic calculations are isotropic, although anisotropy may be added in the near future. Calculations can be done on a single workstation, on a workstation cluster, or on a massively parallel processing system (MPP), depending on the requirements of the problem. The calculations described here were run on a medium-scale parallel system, an SGI Origin 2000, and on a PC-cluster system.

The SEG/EAGE salt velocity model contains compressional wave velocity (Vp) values defined on a 20 m grid of 676 by 676 by 210 elements. This covers model dimensions of 13.5 km by 13.5 km by 4.18 km in depth. To reduce both the memory and computing time needed, the SEG/EAGE acoustic wave calculations used a compute grid with ½ the lateral (X and Y) extents of the full model grid, and full depth extent. This compute grid was thus ¼ the size of the full model grid.

Elastic numerical calculations require shear wave velocities (Vs), and densities (ρ) as well as compressional wave velocities (Vp). We used the same Vp values as were used by the SEG/EAGE acoustic calculations and derived Vs and ρ from them. A table of Vp/Vs values that approximates a velocity-depth trend appropriate for the Gulf of Mexico was devised

Table I, Vp/Vs vs Depth	
Depth, km	Vp/Vs
0.0 (if water)	∞ (Vs=0.0)
0.0 (if sediments)	5.0
0.6	3.5
1.5	3.0
3.0	2.5
4.5	2.3
6.0	2.0
Salt (all depths)	1.9

(Table I; L. Thomsen, personal communication, 1988); the Vp/Vs ratio at a given depth was interpolated from the table. The relation used to derive the density of the sediments in the model was (Gardner, et.al., 1974):

$$r = 0.23 * (Vp)^{1/4} \quad (1)$$

In this equation, ρ is density (g/cm^3) and Vp is p wave velocity (Ft/s). The density of the salt portions of the model was taken as a constant, 2.2 g/cm^3.

The lowest shear wave velocity values are much lower than the lowest compressional wave velocities. That means that shear waves have correspondingly shorter wavelengths than compressional waves. In turn, the spacing of the velocity grid had to be finer to avoid contamination by numerical dispersion in the numerical simulations. We interpolated the original 20 m velocity grid to a 12 m interval using a tri-liner interpolator. The finer grid spacing produced a velocity model that was larger, and requires more memory and more computation time. The interpolated model has 1126 by 1126 by 349 grid points and the interpolated Vp, Vs, and density model files each occupy about 1.7 gigabytes of disk space. We used a subset of the full velocity model, the compute grid, similar to the scheme used by the SEG/EAGE modeling project. The lateral extents of the compute grid are half the those of the full model grid, and the depth extent includes the entire depth of the full model. The horizontal center of the compute grid was placed at the location of each shot. Shots were shallow (12 m below the water surface).

We defined a grid of shot locations that covers almost the entire salt body of the SEG/EAGE model with a shot spacing of 480 m (Figure 1). Two types of receiver arrays were used. One simulated traditional one-component (1C) marine recording with hydrophones. The other simulated a four-component (4C) ocean bottom cable (OBC) survey with each receiver group containing a hydrophone as well as a three-component set of geophones. The marine recordings consist of 4 separate surveys, corresponding to 4 different sailing directions. Each survey contained 8 streamers, at lateral spacing of 80 m. Each streamer had 141 groups with a group interval of 24 m. Two ocean bottom surveys were laid out, with cables aligned perpendicularly (in the X and the Y directions - top to bottom and left to right, respectively, in

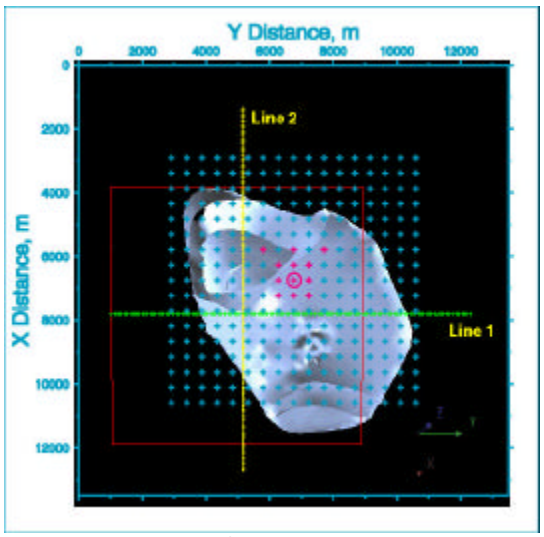

Figure 1. Map view of shot grid used (crosses); shots are at a spacing of 480 m. Shots in purple were computed; shot 145 is circled. Underlying image is the top surface of the salt body in the SEG/EAGE model.

Figure 1). The cables were fixed for all shots, but only receivers within the compute grid were calculated. Since the compute grid was centered on the shot location, the set of OBC receivers was slightly different for each shot. Each

ocean bottom survey contained a total of 14 cables, spaced at 996 m, of which 6 lay within the compute grid for each shot. Each of the 14 cables contained a total of 651 4C groups with a group interval of 24 m, of which 281 groups were active for each shot.

Examples

The computing time that was available was enough to compute elastic data from only 12 shots (Figure 1). In addition, acoustic-only data were computed for one shot, shot 145 (it is circled in Figure 1. Figure 2 shows the velocities, Vp at top, Vs at bottom, in a vertical section of the 3-D velocity structure through the location of shot 145. This is a vertical section from top to bottom of Figure 1.

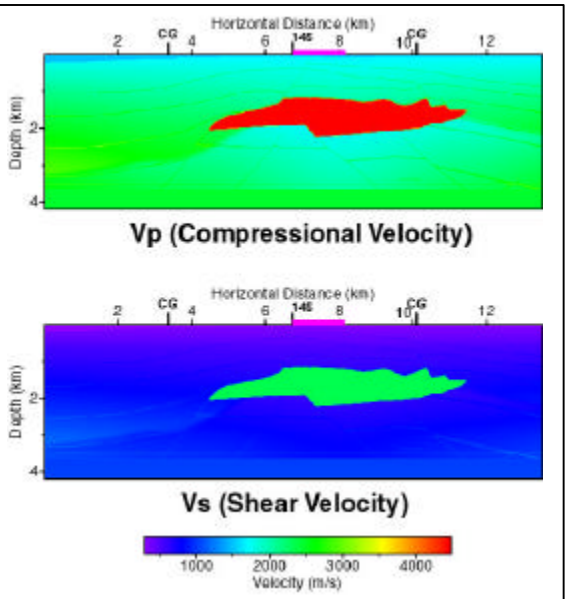

Figure 2. Vertical cross sections through compressional wave (top) and shear wave (bottom) velocity structure. The red and green bodies in the central portions of the top and bottom plots, respectively, are salt. Position of shot 145 is indicated by a labeled vertical bar, the extent of the traces plotted in Figure 3 by a magenta bar, and the limits of the compute grid by vertical bars labeled "CG".

The elastic computations for the 14 shots required a total of 3,375 CPU hours on an SGI Origin 2000 system, an average of 281 CPU hours per shot. Computations used 16 of the system's 96 CPUs (CPU's were 250 MHz R10000). Although the 16 CPUs were supposed to have been dedicated to these calculations, the times to compute individual shots varied by a factor of 4, perhaps because of competition with other processes for I/O. The computations required about 6.2 gigabytes of system memory.

We used Message Passing Interface (MPI) explicit message passing for the computations. We also tried the auto-threading option available in the compiler, but found MPI ran considerably faster. Another potential performance improvement would be to test different ways of decomposing the parallel portions of the calculations to find the best decomposition for the Origin 2000. We have seen as much as 50% performance improvement on other systems by using more optimal parallel decomposition. We did not have the time or computing available to test different decompositions, so used a simple decomposition that has performed acceptably, if not optimally, on other systems.

Because of the great current interest in computing on PC clusters, we carried out similar calculations on a 16 CPU cluster that used 600 MHz Pentium III CPUs. These calculations required about 304 CPU hours, not much more than the Origin 2000. We note that the cost of computing on the PC cluster would probably be less than 1/2 that of the Origin 2000.

Three shot gathers of the near 60 traces of one 4C (four-component) group from an ocean bottom cable are shown in Figure 3. The left portion is a plot of the P-wave (hydrophone component) from the acoustic-only computation. The center plot is the P-wave component from the elastic computation. The right plot is a horizontal geophone component (aligned in the Y direction - to the right on Figure 1) from the elastic computation. The ocean bottom cable was aligned along the Y direction (up-down in Figure 1), and was positioned 480 m from the shot in the Y direction (right in Figure 1). Thus, although these are the 'near' 60 traces in terms of X position relative to the shot, they were recorded from positions offset 480 m laterally from the shot. The traces in the left plot show a direct arrival at a time of about 0.3-0.4 s on the nearest traces (labeled "D" in Figure 1). Beneath that, at times of about 0.75 and 1.0 s are small amplitude reflections from the two interfaces above the salt body (R1, R2). Larger amplitude events at about 1.4 and 1.7 s are reflections from the top and the base of the salt body (T, B). There are few obvious coherent events below the base of salt reflection. The P waves from the elastic calculations in the center plot are similar those from the acoustic calculations, but with a few differences are notable. The nearest offset traces from the top of salt reflection (T) have similar amplitude and waveform character, but the far offset traces are fairly different, presumably because of P to S conversion that is not modeled in the acoustic case. The event at about 2.0 s, especially on the middle offset traces, is probably a salt interbed multiple. Below about 2.0 s, there are few coherent events. The horizontal geophone gather (Figure 3, right) is more difficult to interpret than the P-wave gather. The upper 1.5 s has similar events to those on the hydrophone component although they are smaller in amplitude. The strong event at about 2.7 s is at about the right time for a salt body converted arrival. This would be a PSSP phase - a P wave down to the salt, converted to an S wave at the top of salt, reflected from the bottom of salt, and converted back to a P wave at the top of salt. The event slightly after 4.0 s is almost as large as the PSSP event, and may be an interbed salt multiple. This would

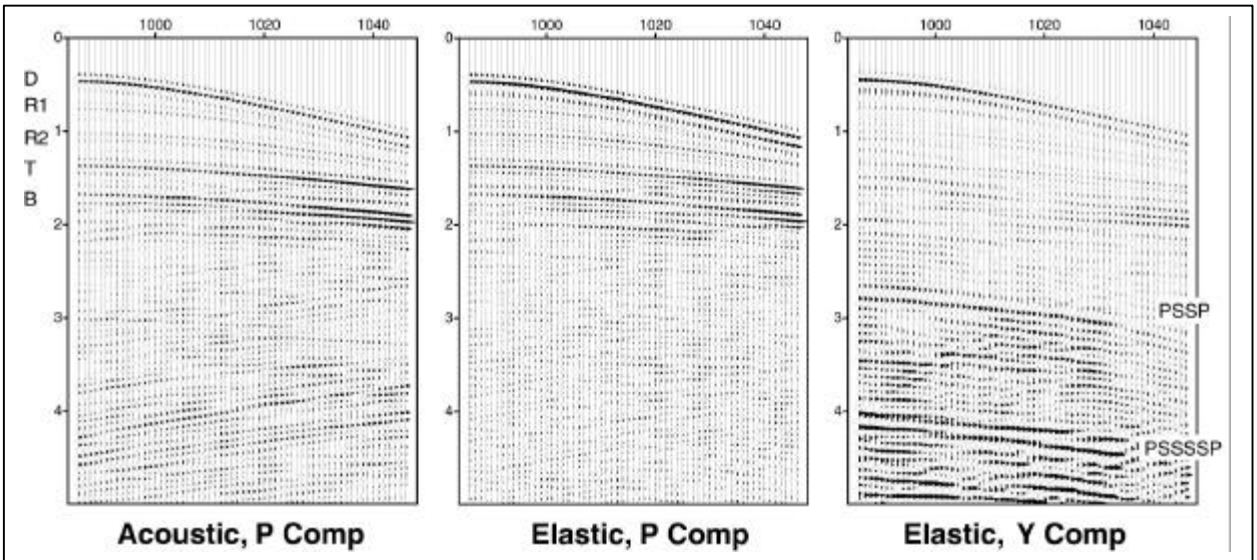

Figure 3. Shot gathers from shot 145, acoustic and elastic calculations. Plots show near 60 traces from a portion of one cable of a 4C ocean bottom cable survey. Additional details are in the text. Hydrophone (P wave) traces from acoustic and elastic calculations are at the left and center, respectively, and transverse geophone traces from elastic calculations are at the right. Labels for reflection events are described in the text.

be a PSSSSP event in the nomenclature used earlier. Neither of these converted wave events (PSSP or PSSSSP) can be seen on the hydrophone gather. There are many smaller, less coherent events in the lower 2 s portion of the transverse geophone traces that may result from multi-pathing within the salt body. Both the top and bottom surfaces of the salt in the model are irregular, and could produce small amplitude events that are difficult to interpret. There is a small amplitude event near the bottom right of the plot that has inverse moveout. This may be real, although there is no obvious feature in the velocity structure that could produce such an event at that time, so it could be a computational artifact.

Conclusions

3-D elastic numerical calculations from the SEG/EAGE salt structure show the importance of modeling to understanding elastic wave propagation effects in a complicated structure. They also illustrate the greater complexity of seismic events that are likely to be in real seismic data from complex structures with large velocity contrasts. These complexities create difficulties for both interpretation and routine processing and imaging, as they result from combined P wave and S wave propagation and interactions with the 3-D geometry of the salt body in this model. The elastic wave calculations also show different amplitudes as a function of offset.

More computations are needed to fully understand the effect of elastic wave interactions with complicated structures. The examples shown here were computed on one system; additional computations on other types of systems, both MPP and clusters, will help to show the relative costs and benefits of different solutions to the computing problem.

Acknowledgments

Leon Thomsen, and Walter Kessinger provided helpful advice and discussions. This work was performed under the auspices of the U.S. Department of Energy by the University of California, Los Alamos National Laboratory, under contract No. W-7045-ENG-36, and Lawrence Livermore National Laboratory, under contract W-7045-ENG 48.

References

Aminzadeh, F., J. Brac, and T. Kunz, 1997, 3-D salt and overthrust models, SEG/EAGE 3-D Modeling Series, No. 1, Soc. Expl. Geophys. Tulsa, OK.

Gardner, G.H.F., L.W. Gardner, and A.R. Gregory, 1974, Formation velocity and density - the diagnostic basis for stratigraphic traps, Geophysics, 39, 770-780.

Larsen, S., and J. Grieger, 1998, Elastic modeling initiative, part III: 3-D computational modeling, Expanded Abstracts, 68th Annual SEG meeting, p 1803-1806.

Qin, F., J.P. Leveille, J.A. Weigant, S.N. Checkles, B.K. Boslaugh, J. McGinnis, H.S. Sanchez, and J.B. Bednar, 1997, Application of elastic modeling to subsalt interpretation, Expanded Abstracts, 67th Annual SEG meeting, p 1092-1095.